MULTISCALE PATTERNS ON A FREE SURFACE BY TURBULENT WAKE

Yutaro Motoori
Graduate School of Engineering Science
The University of Osaka
Toyonaka, Osaka, 560-8531, Japan
y.motoori.es@osaka-u.ac.jp

Takaya Masuda
Graduate School of Engineering Science
The University of Osaka
Toyonaka, Osaka, 560-8531, Japan
t_masuda@fm.me.es.osaka-u.ac.jp

Augusto H. P. Zanca
Graduate School of Engineering Science
The University of Osaka
Toyonaka, Osaka, 560-8531, Japan
a_zanca@fm.me.es.osaka-u.ac.jp

Susumu Goto
Graduate School of Engineering Science
The University of Osaka
Toyonaka, Osaka, 560-8531, Japan
s.goto.es@osaka-u.ac.jp

ABSTRACT

We experimentally investigate the deformation of a gas–liquid interface due to the turbulent wake behind a cylinder. The cylinder is submerged parallel to the free surface in a circulating open channel. The gap between the free surface and the top of the cylinder is set to be comparable to the cylinder diameter, which leads to turbulent vortices similar to those in the single-phase turbulence. We focus on how these vortices deform the free surface. To this end, we quantitatively measure the surface deformation using the synthetic schlieren technique. In the upstream region just behind the cylinder, large-scale surface patterns parallel to the cylinder appear periodically, whereas streamwise-elongated smaller-scale patterns are formed between the large-scale ones. We show that these multiscale surface patterns are generated by multiscale vortices beneath the surface. More concretely, we demonstrate that large roller vortices shed from the cylinder and small rib vortices developing between the rollers contribute to the deformation. In addition, we measure the propagation speed of the surface patterns, showing that the upstream patterns are advected by the inflow velocity; whereas in the downstream, they are predominantly advected by free-surface gravity waves, indicating that vortices beneath the surface no longer determine the surface pattern there.

INTRODUCTION

In turbulence, different-size vortices coexist. In our previous studies (Goto *et al.*, 2017; Motoori & Goto, 2019, 2021; Goto & Motoori, 2024), we revealed concrete pictures of these vortices in physical space through direct numerical simulations (DNS) of various types of turbulent flows. As an example, figure 1 shows vortices in the wake behind a cylinder obtained by our DNS (Fujino *et al.*, 2023) at a Reynolds number of Re $= 5000$ based on the cylinder diameter. We see that roller vortices (grey) are shed from the cylinder, rib vortices (blue) are created between roller ones, and further smaller vortices (yellow and white) are also created around larger ones. Thus, turbulence at high Re consists of multiscale vortices. Based on these vortices, many researchers have accumulated a significant body of knowledge on single-phase turbulence.

Now, research on turbulence is shifting from single- to multi-phase flows. In the present study, we target turbulence wake behind a cylinder placed under a free surface. In this case, the turbulent wake can deform the free surface and induce coherent patterns. To clarify the origin of the deformation patterns on a free surface, there were many experiments (Kumar *et al.*, 1998; Savelsberg & van de Water, 2009; Qi *et al.*, 2025) and numerical simulations (Aarnes *et al.*, 2025). In the present study, we conduct experiments on turbulent wake behind a cylinder under a free surface, using a circulating open channel. To reveal the relation between multiscale vortices in the wake and the deformation patterns on the free surface, we quantitatively measure the velocity field and the surface deformation using particle image velocimetry (PIV) and the synthetic schlieren method (Moisy *et al.*, 2009), respectively.

EXPERIMENTS

In the experiments, we use a circulating open channel apparatus, which was also used in our previous study (Motoori *et al.*, 2025). Figure 2 shows a schematic of this apparatus. We set a cylinder with diameter $D = 20$ mm at a depth $d = 20$ mm under the free surface. In the following section, we show results for the inflow velocity with $U = 125$ and 210 mm/s. The Reynolds numbers are $\mathrm{Re} = UD/\nu = 2.5 \times 10^3$ and 4.2×10^3, where ν is the kinematic viscosity. Although these values are lower than Re $= 5000$ (figure 1) in the DNS (Fujino *et al.*, 2023), the flow is also turbulent, and roller and rib vortices are developed.

To quantify the deformation of a free surface, we use the synthetic schlieren method (Moisy *et al.*, 2009). As shown in figure 2(b), we set a random dot pattern above the surface, and take its distortion using a high-speed camera below. Using image processing, we quantify the displacement $\Delta\boldsymbol{X}$ of the distorted pattern. Then, we evaluate the local gradient vector $\boldsymbol{G}$ of the free surface from the proportionality of $\Delta\boldsymbol{X} \propto \boldsymbol{G}$, where the proportionality factor is determined by the optical arrangement, the distance between the surface and the dot pattern, and the refractive index. Thus, by measuring $\Delta\boldsymbol{X}$, we can reconstruct the spatial distribution of the gradient vector $\boldsymbol{G}$ of the free surface. We also measure the velocity field behind

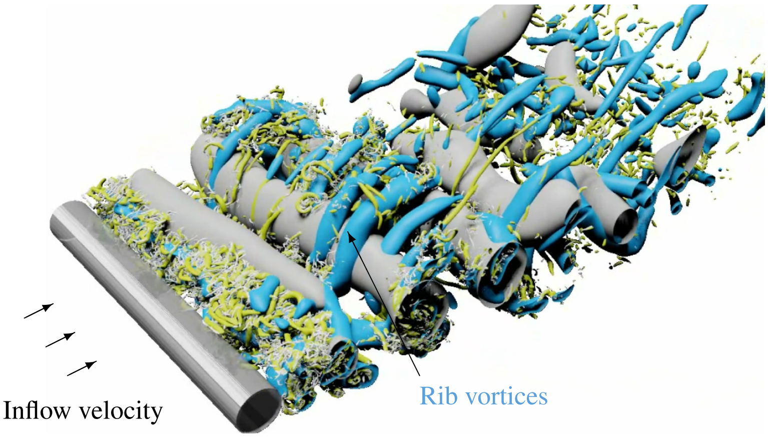

Figure 1. Visualization of vortices in turbulent wake behind a cylinder obtained by our DNS (Fujino *et al.*, 2023). Gray roller vortices are periodically shed from the cylinder, and blue rib vortices are created between roller ones.

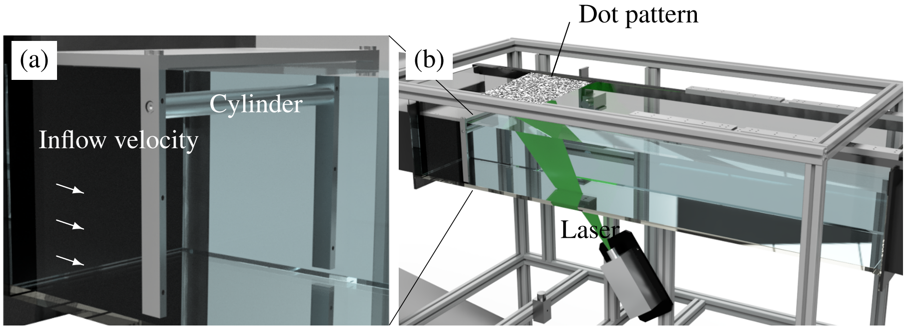

Figure 2. Schematic of the circulating open-channel apparatus. (a) is the magnification of the region around the cylinder in (b).

the cylinder using PIV. Note that the PIV measurement is on the x–z plane (streamwise and vertical directions), whereas the quiescent free surface lies on the x–y plane.

RESULTS

Figure 3(a) shows the velocity field behind the cylinder ($3 \lesssim x/D \lesssim 5$) at $\mathrm{Re} = 2.5 \times 10^3$. Here, the origin ($x = y = 0$) is defined at the downstream edge of the cylinder, with the cylinder center at $x = -0.5D$ and $y = 0$. The arrow colour indicates the sign of the z-directional vertical velocity with upward (black) and downward flows (blue). It is clear to see that a pair of roller vortices is formed on the x–z plane. We emphasize that not only these rollers but also rib vortices are generated in this turbulence, similarly to figure 1. In the following, we focus on the contribution of these multiscale vortices to the deformation of the free surface.

Figure 3(b) shows the spatial distribution of the free-surface gradient vector $\boldsymbol{G}$ behind the cylinder. The arrows point in the direction of decreasing free-surface height; that is, vector sources correspond to crests, whereas sinks correspond to troughs. Around $x/D \approx 5$ in figure 3(b-i), we can observe a large-scale sink extending in the y direction. This deformation pattern can be created due to roller vortices existing beneath the pattern. Indeed, when looking again at the velocity field at the same instant and location shown in figure 3(a), we find that the downward velocity (blue) due to the roller vortices coincides with the position of the large-scale sink.

It is also interesting to observe that not only the rollers but also rib vortices contribute to the free-surface deformation. In figure 3(b-i), we can see that a small-scale source appears in the region for $3 \lesssim x/D \lesssim 4$. Figure 3(b-ii) also shows the spatial distribution of $\boldsymbol{G}$ at a later time than (a), where an array of three sources is aligned in the y direction. In this region ($3 \lesssim x/D \lesssim 4$), a stretching field is induced between a pair of roller vortices [see figure 3(a)], and according to our DNS results (Fujino *et al.*, 2023), rib vortices are created due to this vortex stretching (see figure 1). In other words, the small-scale patterns are likely to be formed by rib vortices. In summary, multiscale deformation patterns appear on the free surface, and their formation is due to multiscale vortices[1].

However, the behaviour becomes more complex in the downstream because the surface patterns formed in the upstream propagate as waves. In other words, surface patterns are determined by the competition between vortices and waves in the downstream. Figure 4 shows the gradient vector $\boldsymbol{G}$ of the free surface at $\mathrm{Re} = 4.2 \times 10^3$ for four streamwise locations [(a)–(d)]. In the most upstream, anisotropic deformation patterns are formed by roller and rib vortices, but they become more isotropic further downstream. We have also confirmed that the advection velocity of the free surface becomes independent of the mean flow velocity, but it is governed by the propagation velocity of free-surface gravity waves.[2]

---

[1]In this experiment, the Froude number is $\mathrm{Fr} = U/\sqrt{gd} = 0.28$ and the Weber number is $\mathrm{We} = \rho D U^2/\sigma = 4.3$ (ρ is the fluid density and σ is the surface tension). This means that in the upstream, the flow inertia (and gravity) can contribute to the free-surface deformation, but the surface tension contributes less. This explains the reason why clear deformation patterns are formed by vortices in the present experiments.

[2]We quantify the advection velocity by evaluating the spatio-temporal correlation of the x-component G_x of the gradient vector:

$$C(r_x, \tau) = \frac{\langle G_x(x + r_x, t + \tau)\, G_x(x,t)\rangle}{\langle G_x(x,t)^2\rangle} \qquad (*)$$

(figures are omitted in this manuscript). In the upstream regions corresponding to those in figure 4(a) and (b), the correlation C takes its maximum at the advection corresponding to the inflow velocity U, which means that the free surface is advected by U. In contrast, in the

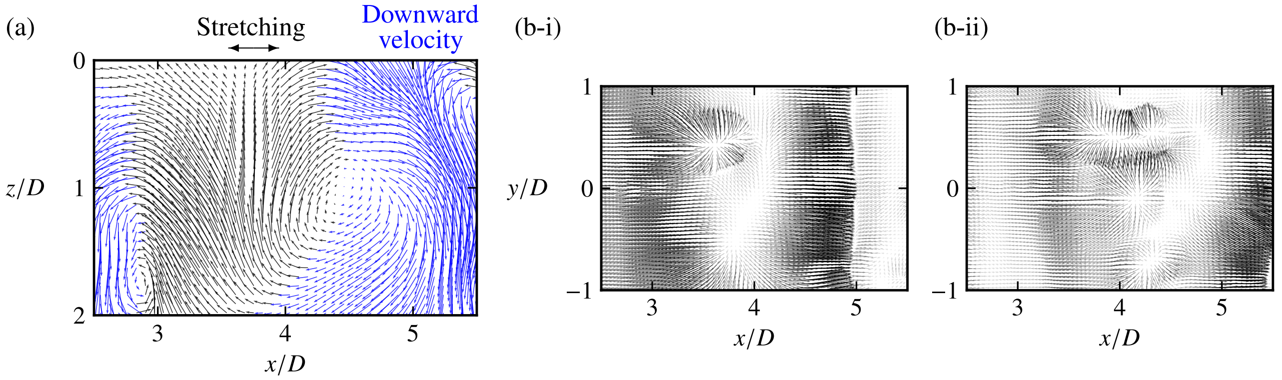

Figure 3. (a) Velocity field on the x–z plane. The blue arrows indicate the downward vertical velocity. (b) Spatial distribution of the free-surface gradient vectors $\boldsymbol{G}$ at Re $= 2.5 \times 10^3$. The time of (b-i) is the same as that of (a). We see that large-scale deformation pattern is formed around $x/D \approx 5$ due to the downward velocity induced by the roller vortices. (b-ii) is a later time than (b-i). We see an array of three sources around $x/D \approx 4$, which are formed by rib vortices.

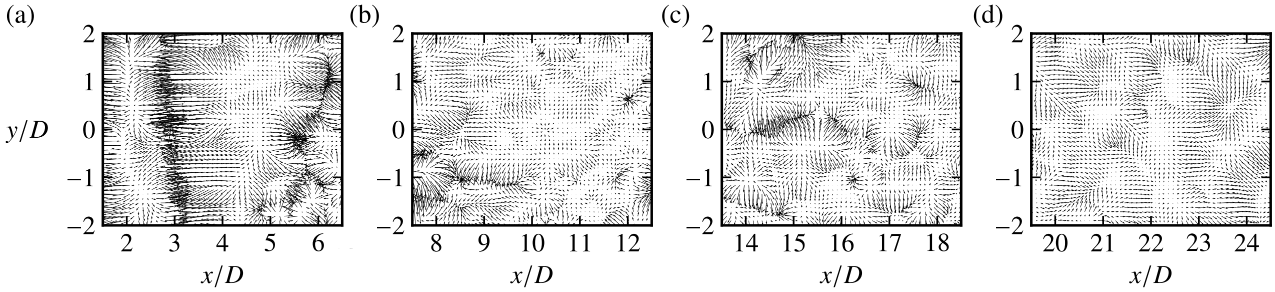

Figure 4. Spatial distribution of the free-surface gradient vectors $\boldsymbol{G}$ at Re $= 4.2 \times 10^3$. The deformation patterns become more isotropic for further downstream [(a)–(d)].

CONCLUSIONS

We have experimentally investigated the free-surface deformation due to the cylinder wake using a circulating open-channel apparatus (figure 2). In the upstream, large-scale patterns are elongated parallel to the cylinder while small-scale streamwise-elongated patterns are formed between the large-scale ones [figure 3(b)]. These multiscale patterns are formed by multiscale vortices beneath the free surface [figure 3(a)]. Further downstream, however, the surface patterns become more isotropic (figure 4). This indicates that in the upstream, vortices beneath the free surface contribute to the formation of the patterns, whereas in the downstream, the free-surface gravity waves become dominant. In the presentation, we will also explain this transition by showing results for the evaluation of (*) in the footnote. In addition, we will show quantitative results for the relationship between surface patterns and multiscale vortices.

ACKNOWLEDGEMENTS

This study was partly supported by the JSPS Grants-in-Aid for Scientific Research (23K13253, 25K01158 and 26K17306) and Grant-in-Aid for Transformative Research Areas (JP26H00389).

downstream [figure 4(c) and (d)], C takes its maximum at the advection corresponding to the summation of U and the free-surface gravity wave velocity U_{wave} $\left(= \sqrt{\frac{g}{D} + \frac{\sigma}{\rho} D}\,\right)$. Thus, the upstream surface patterns are formed mainly by multiscale vortices beneath the free surface, while in the downstream, the free-surface gravity waves become significant.

REFERENCES

Aarnes, J. R., Babiker, O. M., Xuan, A., Shen, L. & Ellingsen, S. Å. 2025 Vortex structures under dimples and scars in turbulent free-surface flows. *J. Fluid Mech.* **1007**, A38.

Fujino, J., Motoori, Y. & Goto, S. 2023 Hierarchy of coherent vortices in turbulence behind a cylinder. *J. Fluid Mech.* **975**, A13.

Goto, S. & Motoori, Y. 2024 Hierarchy of coherent vortices in developed turbulence. *Rev. Mod. Plasma Phys.* **8**, 23.

Goto, S., Saito, Y. & Kawahara, G. 2017 Hierarchy of antiparallel vortex tubes in spatially periodic turbulence at high Reynolds numbers. *Phys. Rev. Fluids* **2**, 064603.

Kumar, S., Gupta, R. & Banerjee, S. 1998 An experimental investigation of the characteristics of free-surface turbulence in channel flow. *Phys. Fluids* **10** (2), 437–456.

Moisy, F., Rabaud, M. & Salsac, K. 2009 A synthetic schlieren method for the measurement of the topography of a liquid interface. *Exp. Fluids* **46** (6), 1021–1036.

Motoori, Y., Fujishima, A., Goda, S., Masuda, T. & Goto, S. 2025 Hydraulic hysteresis in turbulent wakes under a free surface. *Phys. Fluids* **37**, 101701.

Motoori, Y. & Goto, S. 2019 Generation mechanism of a hierarchy of vortices in a turbulent boundary layer. *J. Fluid Mech.* **865**, 1085–1109.

Motoori, Y. & Goto, S. 2021 Hierarchy of coherent structures and real-space energy transfer in turbulent channel flow. *J. Fluid Mech.* **911**, A27.

Qi, Y., Li, Y. & Coletti, F. 2025 Small-scale dynamics and structure of free-surface turbulence. *J. Fluid Mech.* **1007**, A3.

Savelsberg, R. & van de Water, W. 2009 Experiments on free-surface turbulence. *J. Fluid Mech.* **619**, 95–125.